Available online at www.sciencedirect.com
ScienceDirect
Journal of Nuclear Materials 377 (2008) 115–121
journal of nuclear materials
www.elsevier.com/locate/jnucmat

Tensile properties of ferritic/martensitic steels irradiated in STIP-I

Y. Dai *, B. Long, Z.F. Tong

Spallation Neutron Source Division, Paul Scherrer Institut, 5232 Villigen PSI, Switzerland

Abstract

Specimens of ferritic/martensitic (FM) steels T91, F82H, Optimax-A and the electron beam weld (EBW) of F82H were irradiated in the Swiss spallation neutron source (SINQ) Target-3 in a temperature range of 90–370 °C to displacement doses between 3 and 12 dpa. Tensile tests were performed at room temperature and the irradiation temperatures. The tensile test results demonstrated that the irradiation hardening increased with dose up to about 10 dpa. Meanwhile, the uniform elongation decreased to less than 1%, while the total elongation remained greater than 5%, except for an F82H specimen of 9.8 dpa tested at room temperature, which failed in elastic deformation regime. At higher doses of 11–12 dpa, the ductility of some specimens recovered, which could be due to the annealing effect of a short period of high temperature excursion. The results do not show significant differences in tensile properties for the different FM steels in the present irradiation conditions.

1. Introduction

High-chromium ferritic/martensitic (FM) steels, as compared with austenitic stainless steels, have higher strength at elevated temperatures up to about 500 °C, better thermal mechanical properties and superior resistance to irradiation induced creep and swelling under a neutron spectrum. They are, therefore, selected for applications in spallation targets with high proton fluxes [1,2].

Among the different types of FM steels, the 7–9Cr FM steels are considered better than those with higher (10–13 wt%) chromium contents because of their lower ductile–brittle transition temperature (DBTT) shifts after neutron irradiation [3,4]. Moreover, the so-called reduced activation FM steels (RAFMS) with 7–9Cr and 1–2W demonstrated further reduction in DBTT shift after irradiation [5,6]. They are, therefore, considered as tentative materials for applications in different nuclear facilities such as fusion reactors and spallation targets. In the first irradiation experiment of the SINQ Target Irradiation Program (STIP-I), a number of FM steels were irradiated in a temperature range of 90–370 °C to doses between 3 and 12 dpa. In the present work, the tensile properties of RAFMS, F82H and Optimax-A, and F82H EBW (electron beam weld) have been investigated and compared with conventional FM steels, T91 and EM10 from previous studies [7,8].

2. Experimental

The F82H steel, IEA Heat 974, was obtained from the fusion materials community in the form of a 15 mm thick plate. The steel was normalized at 1040 °C for 38 min and tempered at 750 °C for 1 h. The composition is: 7.87Cr, 1.98W, 0.03Ta, 0.02Ni, 0.003Mo, 0.1Mn, 0.04Ti, 0.19V, 0.002Nb, 0.01Cu, 0.09C, 0.07Si, 0.003P and 0.007N in wt%, balance Fe. The Optimax-A steel was developed by the Fusion Materials Technology Group of Federal Poly-technique University Lausanne, Switzerland. The steel was in the form of an 8 mm thick plate. It was normalized at 1050 °C and tempered at 750 °C for 2 h. The composition of the material is: 9.3Cr, 0.97W, <0.01Ni, 0.09Mo, 0.6Mn, 0.24V, <0.01Nb, 0.098C, 0.02Si, 0.01P and 0.055N in wt%, balance Fe. The F82H EBW was prepared from 3.3 mm thick plates. The plates were preheated to about 280 °C. The travel speed was about 10 mm/s. The post-welding heat treatment was performed at 720 °C for 1 h.

* Corresponding author. Tel.: +41 56 310 4171; fax: +41 56 310 4529.
E-mail address: yong.dai@psi.ch (Y. Dai).

0022-3115/$ - see front matter © 2008 Elsevier B.V. All rights reserved.
doi:10.1016/j.jnucmat.2008.02.036

The metallographic inspections of the FM steels [9] illustrate that the size of the prior austenitic gains (PAG) is 70–80 μm for F82H, about 20 μm for Optimax-A. In the fusion zone of the F82H EBW the PAG size is about 30 μm, much smaller than that of base steel. The microhardness of the F82H and Optimax-A steels is similar, about 220 $HV_{0.05}$. For the F82H EBW, it is about 250 $HV_{0.05}$ in the fusion zone.

The tensile specimens are a miniature type originally proposed for the application in the fusion materials community [10]. The dimensions of the specimens are shown in Fig. 1. The specimens were cut along the rolling direction of the plates with an EDM machine, afterwards polished mechanically to the final thickness of 0.4 mm. There were no additional heat treatments before irradiation.

The irradiation was performed in SINQ Target-3 with 570 MeV protons during 1998 and 1999. Detailed information for the irradiation can be found in Ref. [11]. The specimens tested in the present work were placed in Rod 1 and Rod 10 in the target. The specimens in Rod 1 were irradiated in a temperature range of 90–370 °C to a maximum dose of 12 dpa. The irradiation was performed with a total proton current of about 0.85 mA for the first 12 months and about 1.04 mA for the last 2 months of actual beam time. The difference in irradiation temperature in these two periods was as large as 20% of the temperature values. The temperature values reported here are the average values of those in the two periods. Irradiation details for all the specimens used in the present study are given in Table 1, which includes the calculated displacement (dpa), helium (He) concentrations, and irradiation temperatures. It should be pointed out that the He contents were corrected with measured values. The hydrogen (H) concentrations were also calculated. But the measurements demonstrated that the actual H content in a specimen could be much less than the calculated level due to the high mobility of H in steels. Therefore, the H contents are not listed in the table to avoid any misleading. More details of the dpa, He and H calculation are presented in Ref. [12].

Tensile tests were performed at room temperature and approximate irradiation temperatures in flowing Ar gas on a 2 kN MTS machine. The nominal strain rate was $1 \times 10^{-3}\ s^{-1}$. The elongation of a specimen was directly measured from the gauge section using a video-extensometer. After tensile testing, the fracture surfaces of some specimens were observed with a scanning electron microscope (SEM) to identify the fracture mode.

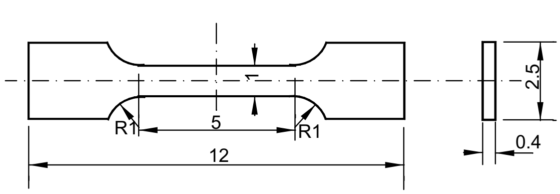

Fig. 1. Sketch showing the dimensions of a tensile specimen.

Table 1
Irradiation conditions and testing temperatures of the specimens tested in the present work

Material	Sample no.	Ti (°C)	Dose (dpa)	He (appm)	Tt (°C)
F82H	P22	85–100 93	3	180	25
	P29	158–187 173	5	350	25
	P03	173–204 188	5.7	370	25
	P10	256–305 280	9.8	815	25
	P11	316–375 345	12	1195	25
	P32	85–100 93	3	178	100
	P37	150–177 164	5	321	150
	P16	137–163 150	5.4	351	150
	P05	173–204 188	5.7	371	200
	P07	261–310 285	9.8	816	300
	P08	275–326 300	9.8	816	350
	P01	321–381 351	12	1195	350
	P02	338–402 370	12	1195	400
Optimax-A	N21	117–137	4.1	250	25
	N12	126–150	5.4	350	25
	N10	181–216	7.6	565	25
	N07	235–280	9.8	815	25
	N05	275–327	11.4	1045	25
	N03	290–344	12	1195	25
	N22	84–100 91	3	178	100
	N11	126–150 138	5.4	351	150
	N23	181/216 199	7.6	567	200
	N25	235/280 258	9.8	816	250
	N04	275/327 301	11.4	1046	300
	N02	290/344 317	12	1195	350
F82H EBW	S17	85–100 93	3	180	25
	S7	186–220 203	5.9	390	25
	S3	214–254 234	7.6	565	25
	S21	186–220 203	5.9	390	200
	S13	214–254 234	7.6	585	250
	S2	260–310 285	9.8	815	300
	S6	313–372 343	11.4	1045	350

Note: the irradiation temperature Ti indicating the range and the mean value of an irradiated specimen.

3. Results and discussion

3.1. Results of the F82H steel

The tensile stress–strain curves of the irradiated F82H specimens tested at room temperature are shown in Fig. 2, including that from an unirradiated specimen. The results indicate the strong hardening and embrittlement effects induced by irradiation at temperatures below about 300 °C. The specimen irradiated to 9.8 dpa and 815 appm He in a temperature range of 255–305 °C failed in elastic deformation regime. The specimen irradiated to 12 dpa with 1195 appm He irradiated in 315–375 °C demonstrated a tremendous increase in yield and tensile strengths and an unexpected recovery of uniform elongation.

The results of the specimens tested at irradiation temperatures are illustrated in Fig. 3. As the irradiation temperature increased with proton flux or irradiation dose, specimens with higher doses were tested at higher temperatures. Due to the effects of higher irradiation and testing temperature, the difference in hardening between specimens

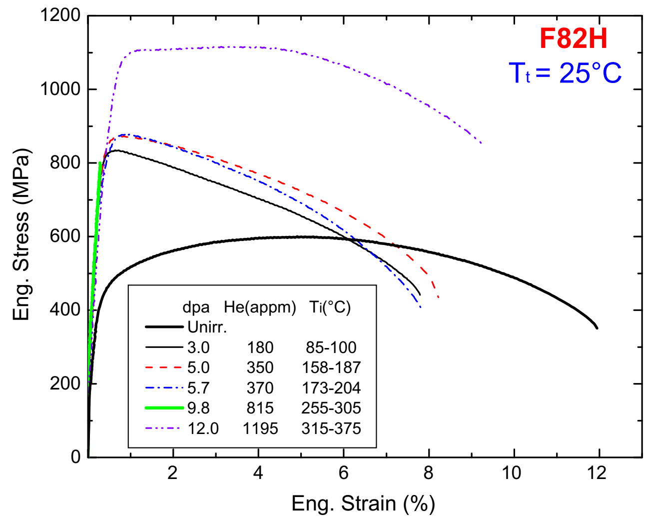

Fig. 2. Engineering tensile stress–strain curves of F82H irradiated in STIP-I and tested at 25 °C.

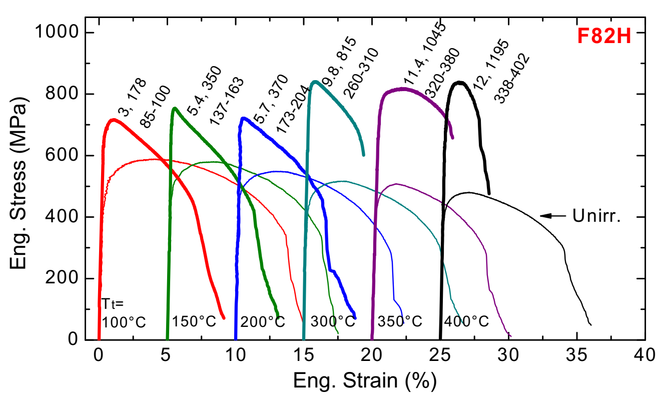

Fig. 3. Engineering tensile stress–strain curves of F82H irradiated in STIP-I and tested at temperatures between 100 and 400 °C. Note: the numbers for each curve indicate the values of dpa, He (appm) and irradiation temperature range.

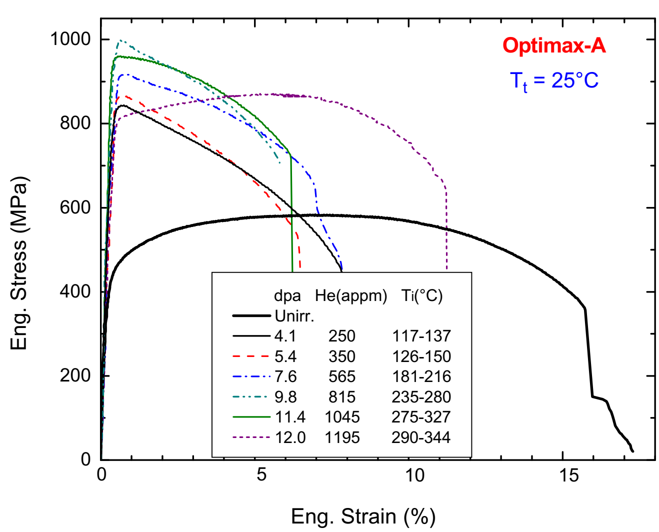

Fig. 4. Engineering tensile stress–strain curves of the Optimax-A steel irradiated in STIP-I and tested at 25 °C.

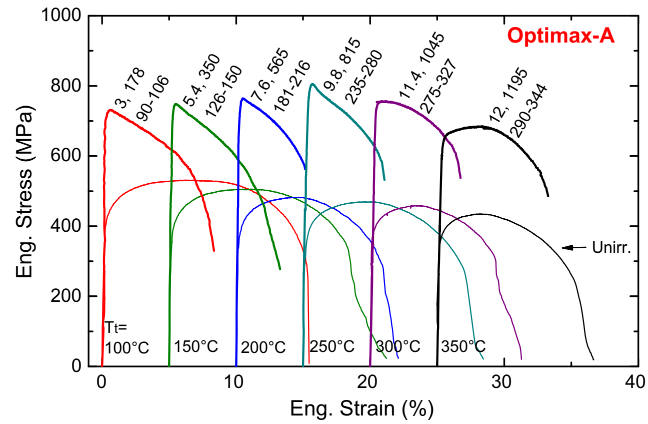

Fig. 5. Engineering tensile stress–strain curves of the Optimax-A steel irradiated in STIP-I and tested at temperatures between 100 and 350 °C. Note: the numbers for each curve indicate the values of dpa, He (appm) and irradiation temperature range.

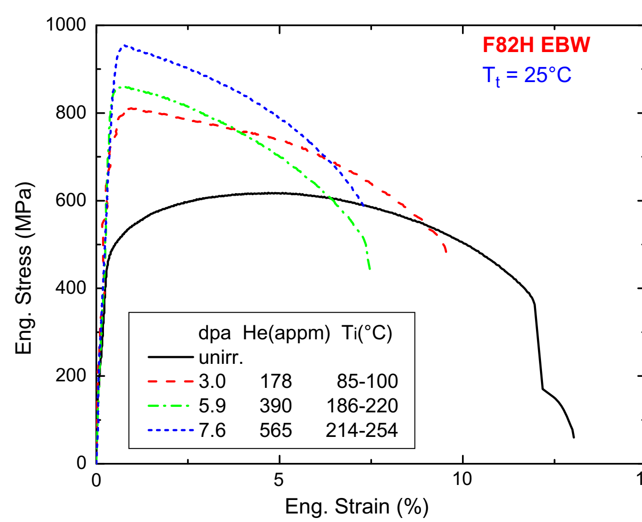

Fig. 6. Engineering tensile stress–strain curves of F82H EBW irradiated in STIP-I and tested at 25 °C.

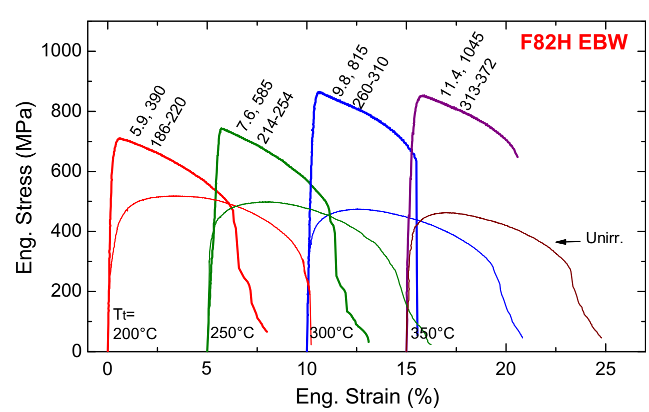

Fig. 7. Engineering tensile stress–strain curves of F82H EBW irradiated in STIP-I and tested at temperatures between 200 and 350 °C. Note: the numbers for each curve indicate the values of dpa, He (appm) and irradiation temperature range.

of higher and lower doses was reduced. Compared to the specimens tested at room temperature, the specimens tested at higher temperatures showed a reduction in strength of 20% or greater. Nevertheless, the hardening and embrittlement effects of the irradiated specimens were still significant, especially for specimens irradiated and tested at ⩽300 °C. However, the specimens irradiated and tested at 350 and 400 °C presented similar uniform elongation values to that of the unirradiated specimens tested at the same temperatures.

3.2. Results of the Optimax-A steel

Results obtained from the tests at room temperature (Fig. 4) indicate that the irradiation induced hardening increases with dose up to 9.8 dpa. The 12 dpa specimen, like the 12 dpa F82H specimen, presented a substantially recovered ductility, but a quite great reduction in strength as compared to the 9.8 dpa specimen.

The results of the specimens tested at irradiation temperatures between 100 and 350 °C are given in Fig. 5. One can see that the results are similar to those of the F82H specimens tested at higher temperatures (Fig. 3). The irradiation induced hardening and embrittlement effects were pronounced for the specimens irradiated and tested at ⩽300 °C. The one irradiated and tested at about 350 °C possessed a uniform elongation similar to that of the unirradiated specimen tested at the same temperature.

3.3. Results of the F82H EBW

The results of the tests performed at room temperature are shown in Fig. 6. It can be seen that the irradiation induced hardening increases with dose, and meanwhile, the ductility significantly decreases. The specimens tested at irradiation temperatures (Fig. 7) show similar behaviors to those of the specimens tested at room temperature, with slightly reduced strength. The specimens always broke outside of the fusion and heat-affected zones as the hardness of the fusion and heat-affected zones was greater than that of the base metal [9].

3.4. SEM observation

Due to high activity of the specimens, as representatives, some F82H specimens were observed with SEM to identify the fracture mode. Fig. 8 shows the SEM micrographs of the fracture surfaces of F82H specimens irradiated to 5.7 dpa and 630 appm He and tested at 25 °C (left column) and 200 °C (right column). Both upper micrographs indicate strong necking before the rupture of the specimens and the micrographs of higher magnifications (middle and lower) illustrate the dimple structure on the surfaces, which indicates typical ductile fracture.

Fig. 9 are the SEM micrographs of the fracture surfaces of the specimens irradiated to 9.8 dpa and 815 appm He and tested at 25 °C (left column) and 300 °C (right col-

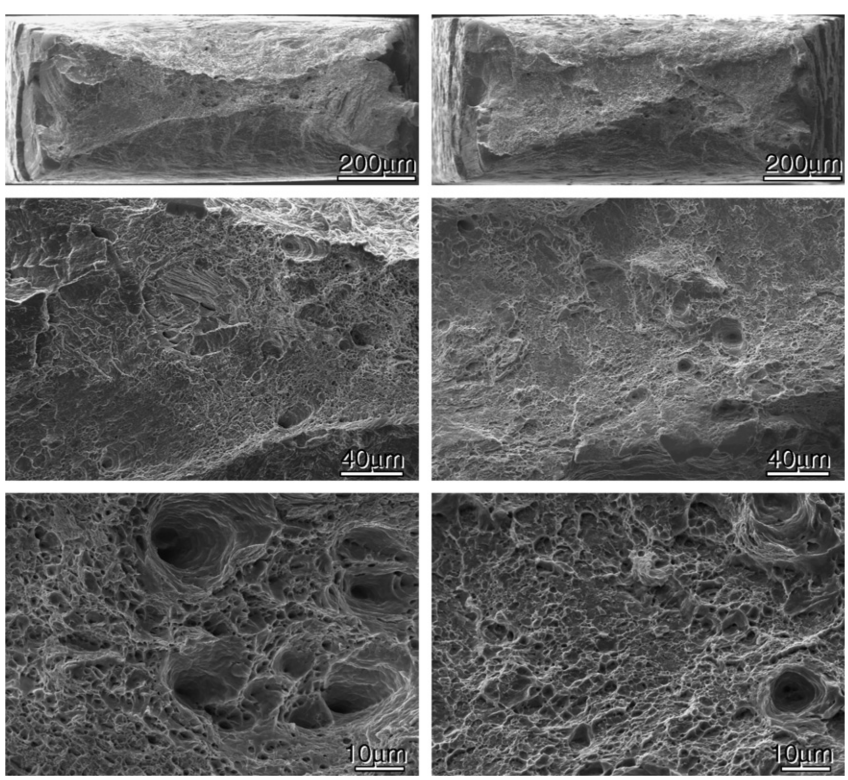

Fig. 8. SEM micrographs showing fracture surfaces of F82H specimens irradiated to 5.7 dpa and 630 appm He tested at 25 °C (left column) and 200 °C (right column).

umn). The graphs in the left column demonstrate that the specimen failed without any necking. The fracture mode is a mixed brittle fracture type of intergranular and trans-granular-cleavage. This is in agreement with the tensile testing results shown in Fig. 2. The pictures in the right column show that the 9.8 dpa specimen tested at 300 °C possesses somewhat cross-section reduction before rupture. However, the cross-section reduction is much less than that

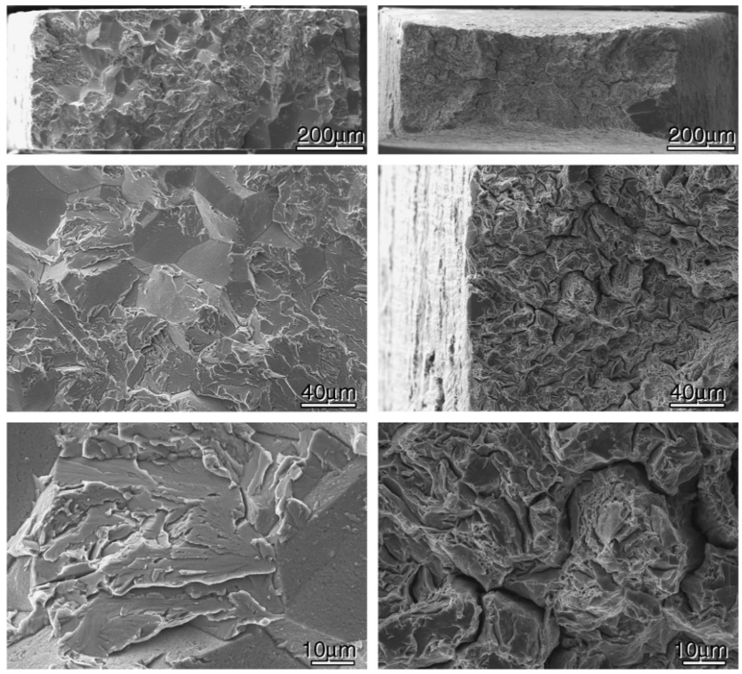

Fig. 9. SEM micrographs showing fracture surfaces of F82H specimens irradiated to 9.8 dpa and 815 appm He tested at 25 °C (left column) and 300 °C (right column).

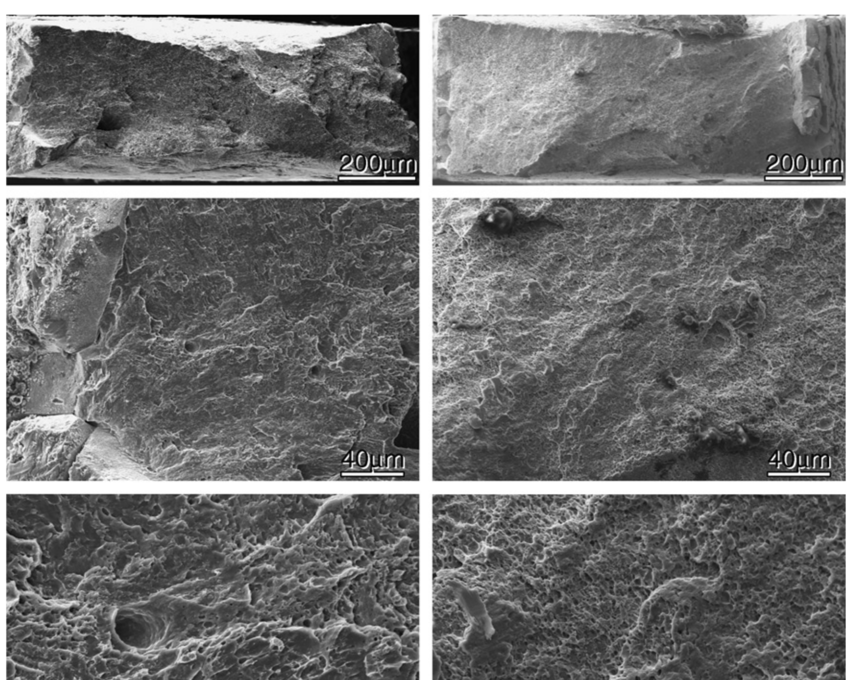

Fig. 10. SEM micrographs showing fracture surfaces of F82H specimens irradiated to 12 dpa and 1195 appm He tested at 25 °C (left column) and 400 °C (right column).

of specimens of 5.7 dpa shown in Fig. 8. Moreover, the fracture mode is transgranular-cleavage although it is not as brittle as the other 9.8 dpa specimen tested at 25 °C.

Fig. 10 shows the fracture surfaces of the 12 dpa specimens tested at 25 °C and 400 °C. Both specimens demonstrate a transgranular ductile fracture mode with dimples, despite of the little cross-section reduction and short elongation of the specimen tested at 400 °C.

3.5. Comparison

The results of the specimens of different FM steels tested at room temperature are plotted in Fig. 11, which shows the dose dependence of YS, UTS, STN and TE. Results from another two FM steels, EM10 [8] and Optifer-V [13], irradiated in the same experiment are also included in the figure. It can be seen that the data from different FM steels fall into a scattering band. In spite of some differences, the data of the different steels show the same trend, especially at doses below 10 dpa. At higher doses around 11–12 dpa, both hardening and embrittlement effects decrease, which are believed to be due to the annealing effects introduced by an unintended high temperature excursion [11].

Fig. 12 presents the results obtained at higher temperatures. The upper figure shows the testing temperature dependence of YS and UTS. For the unirradiated specimens, both YS and UTS decrease with increasing testing temperature, which agrees with general observations (e.g. [14]). For the irradiated specimens, the higher testing temperatures of the specimens of higher doses reduce the difference between the strengths of specimens of different doses. Consequently, the YS and UTS of the different steels remain in a range of about 700–900 MPa under the present irradiation conditions. The lower figure illustrates the testing temperature dependence of STN and TE. The trend, both STN (or UE) and TE decreasing with testing temperature, agrees again with general observations. Under the present irradiation and testing conditions, the STN of the specimens of different steels remains at a low level 1–2%. The TE of the irradiated specimens decreases with testing temperature, which shows a trend similar to that of unirradiated specimens.

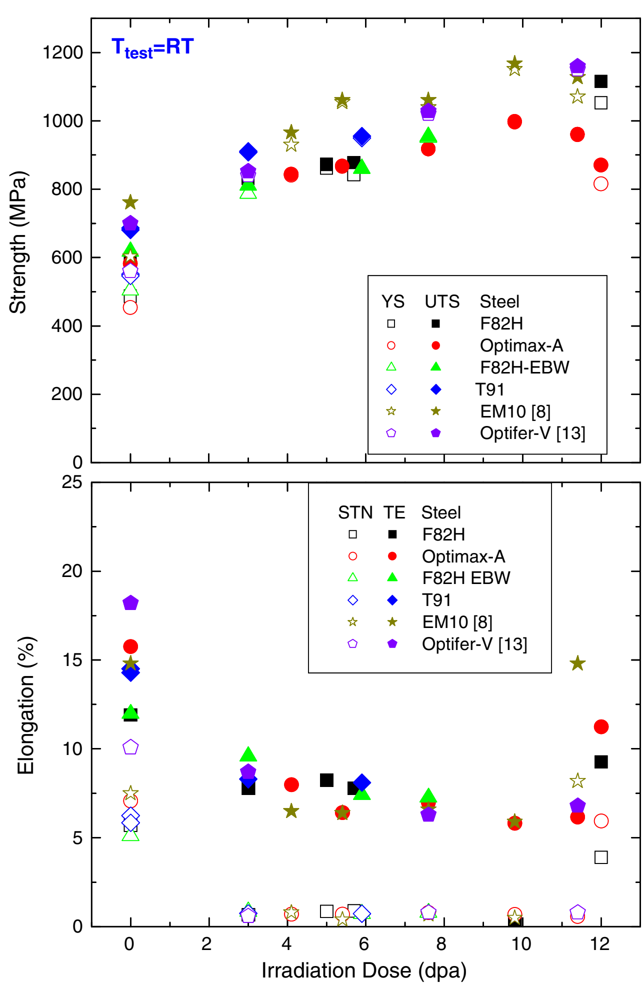

Fig. 11. Irradiation dose dependence of YS and UTS (upper) and STN and TE (lower) of specimens from different FM steels tested at room temperature.

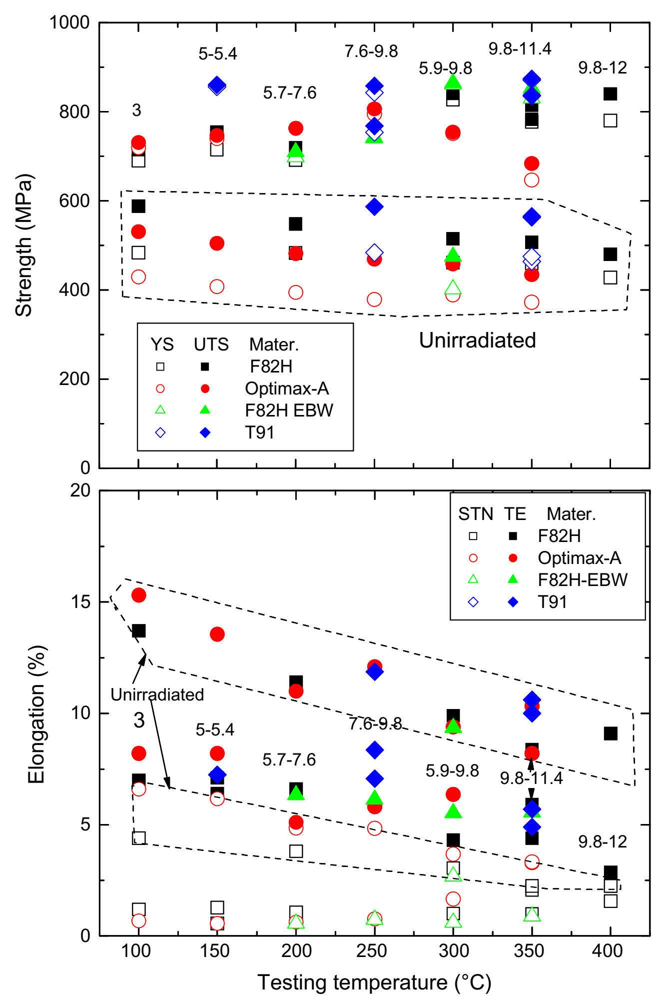

Fig. 12. Testing temperature dependence of YS and UTS (upper) and STN and TE (lower) of specimens from different FM steels irradiated in STIP-I.

From Figs. 11 and 12 one can see that the FM steels demonstrate quite similar tensile properties under present irradiation conditions.

4. Conclusions

Specimens of ferritic/martensitic (FM) steels T91, F82H, Optimax-A and the electron beam weld (EBW) of F82H were irradiated in SINQ Target-3 to doses between 3 and 12 dpa in a temperature range of 90–370 °C. The results of tensile tests demonstrate that:

(a) At $<\sim$10 dpa, the irradiation hardening increases with dose, meanwhile, the embrittlement effect is significant and the uniform elongation decreases to less than 1%. However, the total elongation remains greater than 5%.
(b) At higher doses of 11–12 dpa, the ductility of some specimens recovered, which could be due to the annealing effect of a short period of high temperature excursion.
(c) An F82H specimen irradiated to 9.8 dpa in 250–300 °C and tested at room temperature failed in elastic deformation regime, although the single result could not give a definitive conclusion.
(d) The results of different FM steels irradiated in the same irradiation do not show significant differences.
(e) Specimens tested at a temperature of 350 °C and above after irradiation show a more ductile response than those tested at lower temperatures after irradiation.

Acknowledgments

The authors would like to thank the colleagues of the Spallation Neutron Source Division (ASQ) and the Laboratory for Materials Behaviour (LWV) of PSI for their help on irradiation and testing experiments.

References

[1] Y. Dai, in: Proceedings of ICANS-XIII and ESS -PM4, October 11–19, 1995, PSI, p. 604.
[2] R.L. Klueh, in: Proceedings of First International Workshop on Spallation Materials Technology, April 23–25, 1996, Oak Ridge, p. 3.3.
[3] R.L. Klueh, D.J. Alexander, in: Effects of Radiation on Materials: 16th International Symposium, ASTM STP 1125, 1992, p. 1256.
[4] A. Kohyama, A. Hishinuma, D.S. Gelles, R.L. Klueh, W. Dietz, K. Ehrlich, J. Nucl. Mater. 233–237 (1996) 138.
[5] R.L. Klueh, W.R. Corwin, J. Mater. Eng. 11 (1989) 169.
[6] M. Rieth, B. Dafferner, H.D. Röhrig, J. Nucl. Mater. 258–263 (1998) 1147.
[7] Y. Dai, X. Jia, K. Farrell, J. Nucl. Mater. 318 (2003) 192.
[8] J. Henry, X. Averty, Y. Dai, P. Lamagnere, J.P. Pizzanelli, J.J. Espinas, P. Wident, J. Nucl. Mater. 318 (2003) 215.
[9] H. Zhang et al., J. Nucl. Mater. 377 (2008) 122.
[10] P. Jung, A. Hishinuma, G.E. Lucas, H. Ullmaier, J. Nucl. Mater. 232 (1996) 186.
[11] Y. Dai, G.S. Bauer, J. Nucl. Mater. 296 (2001) 43.
[12] Y. Dai, Y. Foucher, M. James, B. Oliver, J. Nucl. Mater. 318 (2003) 167.
[13] J. Chen, M. Rödig, F. Carsughi, Y. Dai, G.S. Bauer, H. Ullmaier, J. Nucl. Mater. 343 (2005) 236.
[14] A.-A.F. Tavassoli et al., J. Nucl. Mater. 329–333 (2004) 257.